



RESEARCH ARTICLE

A Non-Ionic Gadolinium Complex whose Relaxometric Behavior is Sensitive to the variation of pH. An Experimental and Theoretical Study on Geometry, Bonding Nature of polyaminocarboxylic Ligand and Their Gadolinium Complex

Eduardo M. Rustoy^{1,2,*} and Norberto Raggio¹

¹UMYMFOR, Departamento de Química Orgánica, FCEyN, CONICET-Universidad de Buenos Aires, Pabellón II, Ciudad Universitaria, Ciudad Autónoma de Buenos Aires 1428, Argentina

²Departamento de Ciencias Básicas, Universidad Nacional de Luján, Ciudad de Luján 6700, Argentina

Received: April 25, 2018

Revised: June 12, 2018

Accepted: August 28, 2018

Abstract:

Background:

In addition, the contribution of cyclic structure to the stability of lanthanide complexes has been evaluated on different ligand platforms and some indications of their relative stability are now available. Additionally, it is well known that one of the most important factors to design smart contrast is pH.

Objectives:

The main objectives were to optimize the synthesis of the macrocyclic ligand, using micro-waves. Then study the relaxometric behavior *in vitro*, depending on the pH, of the gadolinium complex and propose a potential structure-activity relationship of the same.

Methods:

The reactions assisted by microwaves were carried out using a Discover[®] CoolMate[™]. Nuclear Magnetic Resonance (NMR) spectra were acquired at 200 and 500 MHz. The Infrared (IR) spectrum of the complex was measured as KBr discs between 400 and 4000cm⁻¹. Electrospray Ionization-High Resolution Mass Spectrometry (ESI-HRMS) was performed on a Bruker microTOF-Q II spectromete-ter. The r1 measurements of the complexes were at 0.2 T, by the inversion recovery method. For the theoretical analysis presented in this work, Hartre- Fock and semiempirical methods were used.

Results:

In the first place, it was possible to carry out the microwave-assisted synthesis of two intermediaries, with higher yields and in a more environmentally friendly way. Then the variation of r1 was checked as a function of the pH value, obtaining a maximum approximately at pH 6.5. The computer tools allowed to propose the possible structures of the coordination compound obtained.

Conclusion:

It was found that the variation of the value of r1 as a function of pH is not a product of the decomposition of the complex, but a stage in which at pH values higher than 7 the complex would undergo a displacement of the water molecule located in the ninth coordination position of the Gd⁺³. This behavior could be due to the replacement of the water molecule by the OH group of the ligand.

* Address correspondence to this autor at the UMYMFOR, Departamento de Química Orgánica, FCEyN, CONICET-Universidad de Buenos Aires, Pabe-llón II, Ciudad Universitaria, Ciudad Autónoma de Buenos Aires 1428, Argentina; Tel/Fax: +54-11-4576-3385; E-mail: erustoy@yahoo.com.ar

Keywords: Gadolinium, Magnetic resonance imaging, Macrocyclic ligand, MOPAC/Sparkle, Longitudinal relaxivity, Infrared.

1. INTRODUCTION

Over the past two decades, Magnetic Resonance Imaging (MRI) has become a very powerful tool in diagnostic medicine [1 - 3]. Paramagnetic materials have been investigated as MRI contrast agents. These materials enhance the contrast of the image indirectly by remarkably shortening the magnetic relaxation time of coordinated water protons as compared with the protons of the surrounding tissues [4 - 6].

The acyclic complex $[\text{Gd}(\text{DTPA})(\text{H}_2\text{O})]^{2-}$ (DTPA= di-ethylenetriamine-N,N,N,N,N-pentaaceticacid), commercially known as Magnevist[®], was the first contrast enhancing agent to be approved for *in vivo* use in MRI [7]. Different $[\text{Gd}(\text{DTPA})(\text{H}_2\text{O})]^{2-}$ derivatives have also been introduced into clinical practice with the aim to improve the properties of the probe [8 - 10].

Janda *et al.* [11] reported the parallel synthesis of macro-cycle **1** (Fig. 1) and developed its Gd(III) complex in conjunction with a parallel screening of these ligands for catalysis of phosphate ester hydrolysis. These authors concluded that the catalytic activity of a family of analogs of compound 1 depends strongly on the identity of the substituent group R. However, they performed no studies to explain this behavior.

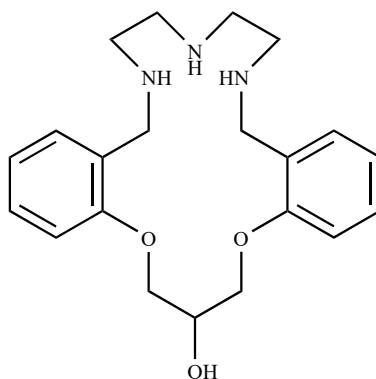


Fig. (1). Molecular structure of macrocycle 1.

Additionally, it is well known that one of the most important factors to design smart contrast is pH [12].

Thus, and because of the decrease in pH observed in hypoxic tissues such as in cancer and metabolic disease, there is a great interest in pH sensors [13].

Among the mechanisms that activate the change in relaxivity depending on the pH of a given contrast agent and that are taken into account in the design of the latter, four are well known whereas others are less known [14].

Based on the above, in the present study, we attempted to establish if the hydroxyl group present in the 1,3-bis(2-methylphenoxy)propan-2-ol residue of the Gd complex recently reported by our group [15], may modulate the relaxometric behavior based on the change of pH of the aqueous medium in which it is dissolved. This may be a new type of potential MRI contrast agent sensitive to changes in pH with low osmotic pressure due to the non-ion characteristic.

As the structure of the $[\text{Gd}(\text{H}_2\text{O})_n]^{3+}$ ($n = 0$ or 1) complex obtained by X-ray is not available, comparisons between the results obtained by the software tools, relaxivity studies, and infrared spectroscopy data were performed. In addition, since the spin-lattice relaxation time (T_1) varies quantitatively as a function of temperature but the equipment used did not allow a temperature control between 30 and 45°C with the precision and accuracy required for such a study, the results of T_1 are mentioned but not quantified. Thus, to study the variation in the longitudinal relaxivity (r_1) of the $[\text{Gd}(\text{H}_2\text{O})_n]^{3+}$ complex as a function of pH, the temperature was set at 37°C.

Additionally, to check that the variation of pH did not lead to the decomposition of the complex in the range studied, *in vitro* studies were performed using a modification of a previously reported method [16].

Finally, we must mention that one of our objectives was to optimize the synthesis of such ligand **2** using microwave irradiation.

2. MATERIALS AND METHOD

All the reactions were monitored for completion by Thin Layer Chromatography (TLC) analyses performed on alumi-num sheets precoated with silica gel 60 (F254). Visualization was accomplished by irradiation with UV light at 254 nm and/or developed in an iodine chamber or by spraying with Dragendorff reagent (bismuth subnitrate-potassium iodide).

Preparative chromatography was performed by elution from columns of silica gel 60. Unless otherwise stated, all the reagents were purchased from commercial sources and used without additional purification (Fig. 2).

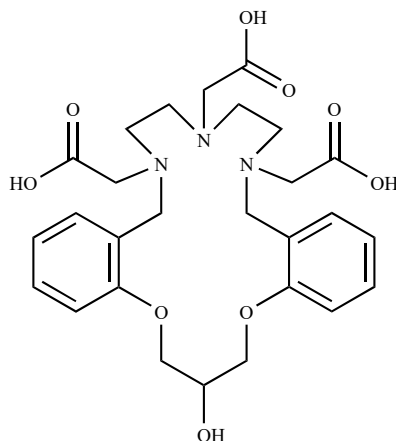


Fig. (2). Molecular structure of macrocycle 2.

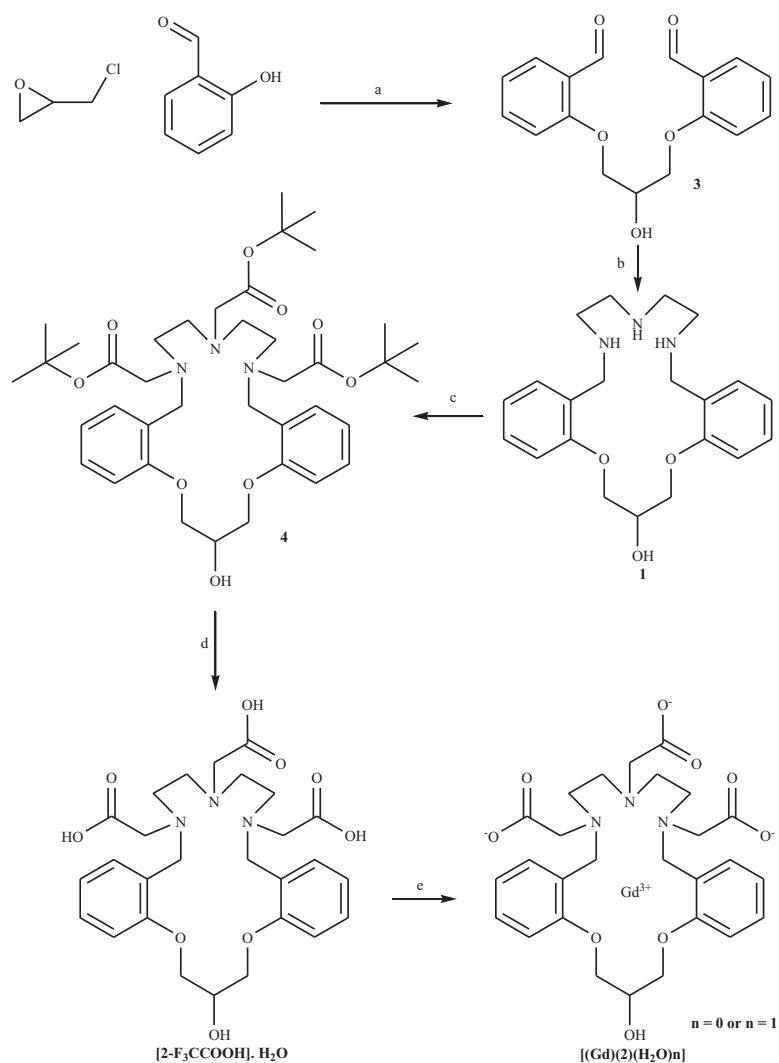
Microwave irradiation was carried out using a Discover[®] CoolMate[™] Low-Temperature Microwave Synthesis System. Nuclear Magnetic Resonance (NMR) spectra were acquired on a Bruker AC-200 (200 MHz) and an Avance II 500 (500 MHz) spectrometer, at room temperature, in CDCl₃ ($\delta = 7.26$ ppm) as an internal standard for ¹H NMR spectra. Chemical shifts (δ) are given in ppm. The Infrared (IR) spectrum of the complex was measured as KBr discs with a Nicolet FTIR Avatar 320 spectrometer. Electrospray Ionization-High Resolution Mass Spectrometry (ESI-HRMS) was performed on a Bruker microTOF-Q II spectrometer. The mass of all the compounds was analyzed by the direct introduction. The isotopic distributions due to the presence of Gd were described by giving the most abundant m/z value of the distribution; the abundance given corresponds to this main peak and is relative to the base peak.

The longitudinal relaxivity (r_1) measurements of the [Gd(2)(H₂O)_n] complex and Gd-DTPA were determined from the spin-lattice relaxation time (T_1). The T_1 values were measured with an NMRT1.0 relaxometer (Unit of Microanalysis and Physical Methods Applied to Organic Chemistry, Argentina) at 10 MHz (0.2 T), by the inversion recovery method. The temperature in the sample holder was kept at 37°C with an air stream.

For the theoretical analysis presented in this work, four different computer programs were used: i) HyperChem 8.0, used for the construction of chemical and pre- optimization of these structures; ii) the Molecular Orbital PACKage (MOPAC) 2012 program, which served to minimize the energy of the proposed structures and obtain the necessary information to predict their infrared spectra, for comparison with the experimental spectrum of the complex; iii) the graphical user interface for computational chemistry software Gabedit 2.4.8, which allowed performing transformations files obtained from calculations performed with the tool packages MOPAC 2012 and HyperChem 8.0; and iv) the tool package Gaussian 09, which was used to calculate the structures of the [Gd(2)(H₂O)_n] ($n = 1$) and **Gd-2** ($n = 0$) complexes.

Procedure for Synthesis of [2-F₃CCOOH]•H₂O and their Gadolinium complex ([Gd(2)(H₂O)_n] ($n = 1$) or Gd-2 ($n = 0$)).

Ligand [2-F₃CCOOH]•H₂O was synthesized by means of a methodology previously reported by us with some modifications [15]. For compounds **3** and **4**, heating by micro-wave was used instead of a conventional heating stage. This tool allowed reducing the reaction times and facilitated the work of purification of the intermediates mentioned (Scheme 1).



Scheme. (1). Reaction Conditions: **a)** microwave irradiation, 120°C, 0.5 h, methanol; **b)** i. Diethylenetriamine, methanol, reflux, 2 h; ii) NaBH₄, 2 h, water, overnight; **c)** t-butyl bromoacetate, N,N-diisopropylethylamine, microwave irradiation, 110°C, 2 h; **d)** i) TFA, dichloromethane, room temperature; ii) diethyl ether; **e)** i) [Gd(NO₃)₃·6H₂O], pH = 7.5-8.0, reflux; ii) acetonitrile, reflux.

Preparation of 1,3-Bis(2-formylphenoxy)-2-propanol (**3**)

A pyrex cylindrical reaction tube was charged with salicylaldehyde (3 mL, 3.45 g, 28.3 mmol), anhydrous K₂CO₃ (340 mg, 2.5 mmol), epichlorohydrin (230 mg, 2.5 mmol), 3 mL of methanol and a magnetic stirrer bar. The tube was septum-sealed and irradiated with microwaves at 120°C for 0.5 h. The temperature was measured by IR detection and maintained constant by modulated irradiation of 300-100W. The reaction mixture was cooled to room temperature, an excess of salicylaldehyde and unreacted epichlorohydrin were evaporated under reduced pressure, and the residue dissolved in CH₂Cl₂ (10 mL) and extracted with water (3x5 mL). The organic phase was dried over anhydrous sodium sulfate. After evaporation of the solvent, the crude product was purified by recrystallization from benzene. 1,3-Bis(2-formylphenoxy)-2-propanol was finally obtained as light yellow needles (547 mg, 1.8 mmol, Yield: 83%). ¹H-NMR (200 MHz, CDCl₃): δ 4.32 (d, 4H, 2(CH₂O)Ph), 4.51 (m, 1H, OCH₂CH₂O), 7.05 (m, 4H, ArH), 7.55 (m, 2H, ArH), 7.80 (m, 2H, ArH), 10.40 (s, 2H, ArCH(O)).

Preparation of Tri-tert-butyl 2,2,2''-(20-hydroxy-7,8,10,11,20,21-hexahydro-5H,19Hdibenzo [1,15,5,8,11] dioxatriazacyclooctadecine-6,9,12-triyl)triacetate (**4**)

A pyrex cylindrical reaction tube was charged with tert-butyl bromoacetate (1.088 g, 5.6 mmol), the crude macrocyclic triamine **1** (0.631 g, 1.7 mmol) in acetonitrile (3 mL) and di-iso-propylethylamine (0.987 g, 7.6 mmol). The

tube was septum-sealed and irradiated with microwaves at 110°C for 2 h. The temperature was measured by IR detection and maintained constant by modulated irradiation of 300–80W. The reaction mixture was cooled to room temperature and the solvent was evaporated under reduced pressure. The residue obtained was purified by chromatography on silica gel (EtOAc/hexane, 9:1 v/v) to give the title compound **4** as a pale yellow oil. (0.809 g, 1.1 mmol, Yield: 67%). ¹H-NMR (500 MHz, CDCl₃): δ 1.44 (m, 27H, COOC(CH₃)₃), 2.95 (s, 4H, NCH₂Ph), 2.70-3.11 (m, 4H, CH₂NBn), 3.11-3.55 (m, 4H, CH₂NCH₂COOC(CH₃)₃), 3.75-4.11 (m, 2H, (CH₂)₂N(CH₂COOC(CH₃)₃)), 4.26-4.42 (m, 4H, CH₂OPh), 4.56-4.64 (m, 1H, CH), 6.80 (m, 4H, ArH), 7.16 (m, 2H, ArH), 7.75 (m, 2H, ArH).

Preparation of 2,2',2''-(20-hydroxy-7,8,10,11,20,21-hexahydro-5H,19H-dibenzo[b,m][1,15,5,8,11]dioxat riazacyclooctadecine-6,9,12-triyl)triacetic acid trifluoro acetate salt, monohydrate [2-F₃CCOOH]·H₂O

Compounds [(2-F₃CCOOH)·H₂O] was synthesized as, and the [Gd(2)(H₂O)_n] (n = 0 or 1) complex were synthesized as described previously [15]. Unlike our previous work, the complex was purified by a Sephadex-50 column eluted with water.

2.1. Relaxometric Measurements

For measurements of the relaxivities r_1 , four different concentrations (0.18, 0.35, 0.7, and 1 mM) of [Gd(DTPA)(H₂O)]²⁻ and [Gd(2)(H₂O)_n] were prepared in tubes. The pH was adjusted from 3 to 8 in one-unit steps by adding solid *p*-toluenesulfonic acid and LiOH, without changing the concentration of the stock solution separately.

To establish whether the variation according to the pH was a dissociation effect of the Gd ion, triplicate samples were incubated for 6, 12, 24 and 48 h. After incubation, the amount of Gd(III) released from the complex was determined at each pH point by eluting a sample through a Se-phadex G-50 column, and comparative measurements were conducted on an identical sample that was not treated in the manner described above. Measurements of the same sample subjected to the change in pH of the medium and the results obtained with those observed for the samples had the same pH but which were not subject to the variation described is performed compared.

Gradient-echo sequence was used to study their r_1 relaxivities with TE = 6 ms and TR = 4, 2 s, 1 s, 200 ms, 150 ms, 100 ms, 50 ms, 25 ms and 18 ms. The background noise effect was removed by subtracting the mean intensity signal with mean intensity signal noise [17].

2.2. Computational Procedure

2.2.1. Studies of **2** and [Gd(2)(H₂O)_n] (n = 0,1)

The geometry of the trianionic (23-) ligand form was further optimized by density functional theory with Becke's three-parameter hybrid method and the correlation functional of Lee, Yang and Parr (B3LYP) with 6-31G(d) basis set [18], without constraints. The atomic charges were calculated using the Natural Population Analysis (NPA) scheme [19]. All calculations were performed with Gaussian09 program package [20].

It should be noted that the formation of compound **2** led to the generation of two stereogenic nitrogens (N₂ and N₄). Single-bonded nitrogen is pyramidal in shape, with the nonbonding electron pair pointing to the unoccupied corner of a tetrahedral region. Since each nitrogen in these compounds is bonded to three different groups, its configuration is chiral, and, due to the presence of the stereogenic centers in compounds **2** and **4**, a mixture of diastereomers will result.

In the absence of the X-ray crystal structure, the ground state geometries of Gd-2 or [Gd(2)(H₂O)] were obtained by molecular mechanics methods, and all the potential starting arrangements of the donor atoms around the Gd(III) metal ion for ligand **2** were considered. For molecular mechanics calculations, the MM+ force field for both complexes was used [21].

The geometries of the complexes were calculated by using the Sparkle/PM6 model implemented in the MOPAC 2012 package [22]. The MOPAC keywords used in all Sparkle/PM6 calculations were: GNORM = 0.01, SCFCRT = 1.D-10 (to increase the SCF convergence criterion), PRE-CISE (the criteria to end all electronic and geometric optimizations are to be increased by a factor, normally 100, using this keyword), EF and XYZ (the geometric optimizations were performed in Cartesian coordinates). To establish whether the structures obtained were consistent with a minimum of energy, the force constants of the vibrational modes were analyzed on the output*.arc files and using the keywords: PM6, SPARKLE, XYZ, AUX (output auxiliary information for use by other programs, for example: GABEDIT 2.4.8 [23]), and FORCE (force-calculation is to be run). The vibrational frequencies, measured by infrared, are

proportional to the square root of the force constants. So, when one of the vibrational force constants is negative, the corresponding vibrational frequency is imaginary. A valid optimized geometry must have all vibrational force constants positive (in which case one can safely say that the geometry is sitting at a true minimum at the potential energy hypersur-face), CHARGE = 0, Singlet (ground state of multiplicity) and LET (which means that the supplied geometry is to be used, even if the gradients are large).

3. RESULTS AND DISCUSSION

3.1. Synthesis of Intermediates 3 and 4

Several methods have been described for the reaction of epichlorohydrin with salicylaldehyde as a precursor for the synthesis of crown ether **1** [24]. In general, all of them consist in two-step processes with pre-formation of the phenoxide salt in basic medium and subsequent addition of epichlorohydrin.

However, microwave irradiation has attracted considerable attention for rapid synthesis of a variety of organic compounds because of the selective absorption of microwave energy by polar molecules [25]. Microwave irradiation has been successfully used in the formation of a variety of carbon-heteroatom and carbon-carbon bonds [26].

During our ongoing efforts to explore organic syntheses using microwave irradiation, we envisioned that the nucleophilic substitution reaction of alkyl halides with amines and phenols might be accelerated by microwave energy because of their polar nature.

In view of the above, we proposed to extend the application range of microwave-assisted methods to the formation of compound **3** by reaction of salicylaldehyde (excess) and epichlorohydrin in the presence of K_2CO_3 without the need of the previous preparation of phenoxide salt and in the absence of dimethylformamide, which was used as solvent in our previous work [15]. The desired product **3** was isolated after purification by recrystallization from benzene with a yield of 83%.

Encouraged by the results obtained in the preparation of compound **3** and based on the same premise as that used in the case mentioned, we thought to apply a similar methodology to obtain polyester **4**. The highest yield was obtained within 2 h of irradiation and applying a maximum power of 300 W. However, after 10 min of reaction, the power stabilized at 80 W, and, working at constant temperature (110°C) and under the conditions described above, we obtained compound **4**, which had a performance similar to that reported by us, but in a significantly shorter time.

3.2. Relaxivity Measurements

The effect of pH on the relaxivity of the two Gd complexes studied was examined at 37°C and 0.2 T (Fig. 3).

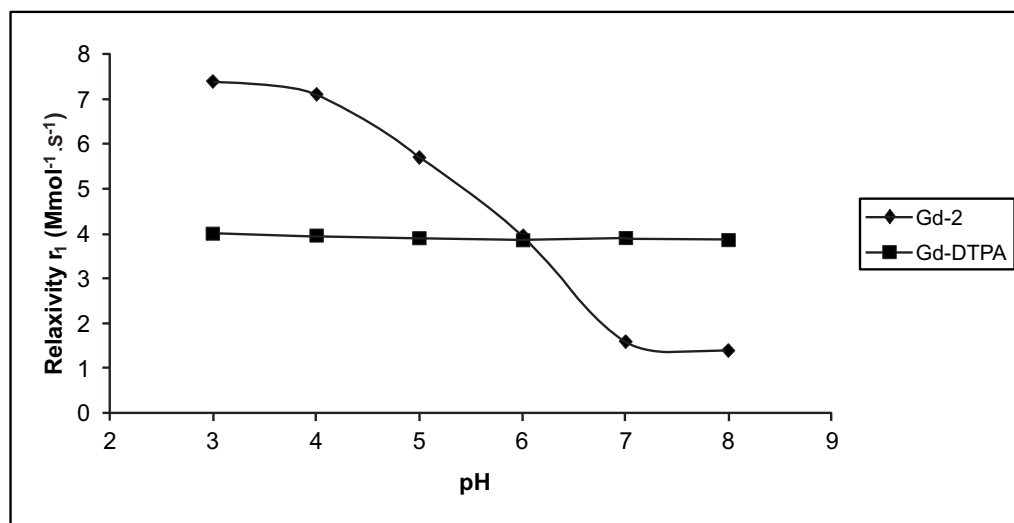


Fig. (3). Variation of relaxivity (r_1) as a function of pH change.

The pH profile of $[\text{Gd}(2)(\text{H}_2\text{O})_n]$ showed a fairly sub-stantial relaxivity enhancement when passing from high to low pH. The inflexion point occurred at a pH of approximately 6.5. The r_1 of $[\text{Gd}(2)(\text{H}_2\text{O})_n]$ increased by 140% from 1.6 to $3.9 \text{ s}^{-1}\text{mM}^{-1}$ (pH 7 to pH 6). This relaxivity enhancement was found to be reversible, and measurements repeated after incubation for 2 days confirmed that the enhancement was not the result of the dissociation of the gadolinium Gd ion. The absence of free Gd (III) ion was confirmed according to the procedure described in the experimental section. The relaxivity pH profile was noticeably different from that observed for $[\text{Gd}(\text{DTPA})(\text{H}_2\text{O})]^{2-}$, which remained flat across this same pH range.

The longitudinal proton relaxivities, r_1 , of $[\text{Gd}(2)(\text{H}_2\text{O})_n]$ and $[\text{Gd}(\text{DTPA})(\text{H}_2\text{O})]^{2-}$ at pH 7-8 fell in the range of values typical of q (number of water molecules coordinated to Gd) 1 and $q = 1$ systems, respectively.

These data indicate that the ligand complex derivative 2 has a 9-coordinate ground state without one inner sphere water molecule [27]. The occurrence of $q = 1$ also included the possible involvement of the OH group of the ligand in the coordination of the metal ion. Accepting the above reasoning would mean recognizing that the variation in acidity relaxation is caused by the variation in the number of water molecules coordinated to Gd, which would be possible only if there were any R-DH functional groups in the ligand ($D =$ any atom capable of yielding a pair of electrons to form part of the coordinating sphere of Gd) that would be protonated ($\text{R}[\text{DH}_2]^+$) at pH below 6.5 (approximately) and which would prevent it from being bound to Gd, obtaining $q = n-1$. In the opposite case, *i.e.* at pH values greater than 6.5, the equilibrium would be displaced towards the R-DH species, where the D atom has the free electron pair available to form a bond with Gd.

An example of the existence of this behavior is that of the complex GdNPDO3A (1-methylene-(p-NitroPhenol) 1,4,7,10-tetraazacycloDodecane-4,7,10-triAcetate) [14]. This contrast agent works by a mechanism similar to that described for the generic agent above. The difference is that, as the nitrophenol group protonates, it dissociates from Gd and allows water access, and thus the effectiveness of the agent is higher at lower pHs.

Based on the above, we may hypothesize that this would not be the mechanism that would take place in our case study since the value of the pKa of the R-OH group present in ligand 2 is much greater than that observed for the nitrophenol group present in the NPDO3A ligand.

The second mechanism takes place when the ligand has hydroxylic protons that can be successfully used to generate chemical exchange saturation transfer when they are close enough to the paramagnetic center. In this sense, it has been reported that the ratiometric value varies in function of the temperature and pH and temperature by the YbHPDO3A (HPDO3A=10-(2-HydroxyPropyl)-1,4,7,10-tetraazacyclo Dodecane- 1,4,7-triAcetic acid)) has been reported [14c]. At this point, it is noteworthy that the measurements of the property in question as a function of the temperature of an aqueous solution containing compound $[\text{Gd}(2)(\text{H}_2\text{O})_n]$ also showed variations and that this phenomenon was reversible. However, as the equipment used does not allow taking measurements with acceptable accuracy, the results are not presented here.

In view of the above and the results obtained by us from spectroscopic and relaxometric data, we decided to perform computational studies that allow us to explain the above experimental evidence and propose possible structures of the $[\text{Gd}(2)(\text{H}_2\text{O})_n]$ complex. To achieve this goal, we also considered necessary to perform a structural analysis of the ligand by using computational tools.

3.3. Computational Studies

3.3.1. Theoretical Studies of the Anionic Form of Ligand 2

The deprotonated form of the ligand was conformationally analyzed in the gas phase by using the molecular mechanics method MM+. The relative energy (stability) orders obtained showed some differences but five conformers always showed comparatively lower energy and were thus selected for the calculations at the higher level of theory (Fig. 4). To simplify the visualization and analysis, structures are presented without the corresponding hydrogen atoms.

It is worth noting that the computational analyses were not performed for the neutral form of the ligand in either solvent or gas phase. The reason for this decision was based on the fact that the objective of these analyses is to establish the O atoms that would present a greater tendency to participate in the coordination of Gd. It is for this reason that, in the calculations made, the water was assumed to be solvent because of its dielectric constant and because, given the low concentrations of the complex used, it is the medium that would present greater similarity to the real reaction

conditions.

Among the many factors that influence the formation or not of a chemical, two of the most important are the steric and electronic effects. To theoretically estimate the incidence of the latter, as mentioned above, the value of the charges was analyzed by the NPA method, which has been developed to calculate the atomic charges and orbital populations of molecular wave functions in general atomic orbital basis sets. This method is an alternative to conventional Mulliken population analysis and seems to exhibit improved numerical stability and to better describe the electron distribution in compounds of high ionic character [19], such as the conformers of ligand 2 in its trianionic form.

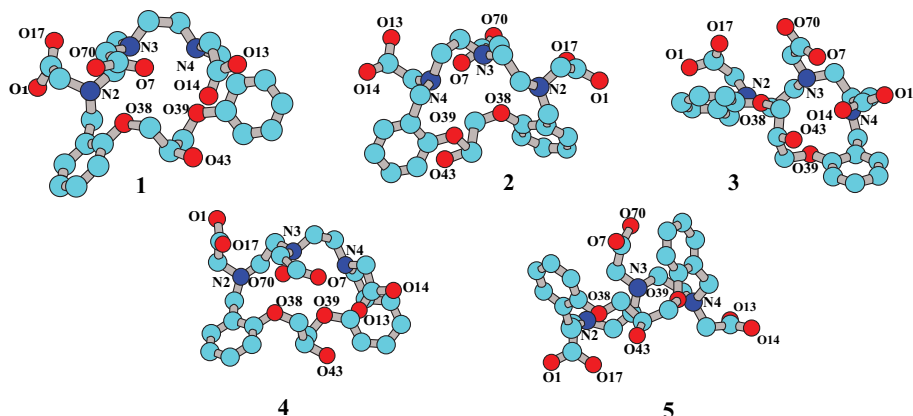


Fig. (4). Geometries of compound 2^{3-} , obtained by search conformational at MM+ level of the theory.

Table 1 shows the values of NPA (q^{NPA}) for the atoms defined as it is required to be observed in Fig. (4).

Table 1. Atomic charges (q , a.u.) at selected atoms in the neutral and deprotonated forms of the ligand 2.

Donor atom	Conformer				
	1	2	3	4	5
	q^{NPA} [a.u.]				
O38	-0.586	-0.575	-0.586	-0.597	-0.598
O39	-0.567	-0.551	-0.515	-0.556	-0.556
O43	-0.795	-0.801	-0.795	-0.802	-0.802
N2	-0.517	-0.507	-0.534	-0.530	-0.535
O1	-0.808	-0.779	-0.800	-0.800	-0.801
O17	-0.802	-0.785	-0.803	-0.807	-0.808
N3	-0.530	-0.530	-0.538	-0.516	-0.530
O7	-0.822	-0.803	-0.807	-0.797	-0.792
O70	-0.802	-0.784	-0.826	-0.804	-0.808
N4	-0.522	-0.510	-0.526	-0.517	-0.530
O13	-0.796	-0.776	-0.806	-0.808	-0.799
O14	-0.805	-0.784	-0.818	-0.815	-0.807

A rapid analysis led to the conclusion that atom **O43** had a greater tendency to interact with the metal center. However, this is only if the electronic factor is taken into account and we do not know the steric hindrance. This is why we decided to study all possible structures of the complex in which oxygen atoms participate [**Gd(2)(H₂O)**] or not [**Gd(2)**].

3.3.2. Modeling of the Structures of the [**Gd(2)**] and [**Gd(2)(H₂O)**] Complexes

There is no unified criterion on how macrocycle **1** coordinates a given metal center (M^{n+}). Some authors indicate that the OH group is involved in the coordination sphere where $M^{n+} = Ni^{2+}$, which was checked by the for obtained structure diffraction X-ray. However, Janda *et al.* represented the same family of complexes with a structure where the OH group was not coordinated, and this information was based on infrared spectroscopy data [28].

In this same sense, these authors observed that when the metal center is Ni^{2+} and the proton of the alcohol group pre-

sent in macrocycle **1** is replaced by a substituent R (R = Me, Bn, β -Naphthyl), the rate of ester hydrolysis increases as the size of R present in the ligand increases. The authors indicated that this would be due to the steric hindrance exerted by the substituent on the probability that the oxygen is coordinated to the metallic center.

Therefore, the interactions between the cation and the carbonyl oxygen atoms of the carboxylic acid groups of ligand **2**, will be more similar to the interactions proposed by Yan *et al.* [29]. They synthesized derivatives ligand **1** where in the N atoms have organic/inorganic hybrid substituents and whose complex derivatives with $M = \text{Eu}^{3+}, \text{Tb}^{3+}, \text{Nd}^{3+}$, are represented by a possible structure where the authors proposed a coordination mode of one Ln^{3+} to two crown ether moieties. In this case, each N-substituted chelating group ($-\text{C}=\text{O}$) is unable to complex the same Ln^{3+} (which is located in the ring of the crown ether molecule) because it is not in an appropriate geometry.

The coordination will thus take place in the inter-molecular mode but not in the intramolecular one [29]. According to the proposed structure, the OH group would not be coordinated to the metal center.

Subsequently, Janda *et al.* [11] carried out a similar study, but using phospho di- and triesters and double-stranded DNA as substrates, and using different Ln^{3+} instead of the aforementioned cations. The authors reached conclusions similar to those of the previous work and provided similar explanations related to the way in which the metallic center is coordinated, depending on the identity of substituent R. Finally, the authors indicated that they would do additional work to study how the metal centers were linked to the different ligands [11, 28]. However, after a detailed bibliographic search, we found no further studies on the way in which the Ln^{3+} cations interact with the ligand. A feature worth noting is the absence of the acetate groups in the structure of ligand **1** compared to that described for compound **2**. This latter characteristic would generate that the structure of the complexes with ligand **1** has fewer restrictions since the groups with negative net electric charge (X^{-}) that confirm the sphere of coordination of the metallic center are not covalently united.

Based on the experimental evidence obtained in the pre-sent study by ESI-HRMS, we can conclude that this last mode of coordination does not explain in finished form since, in addition to the obvious structural differences, the Gd/compound **2** ratio in the **Gd-2** complex would be 1:1 (Fig. 5).

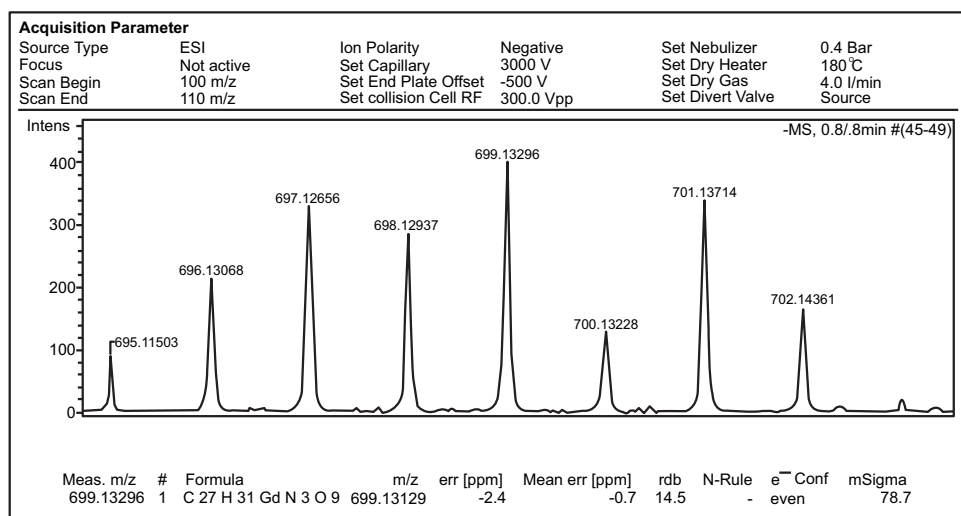


Fig. (5). Region of ion molecular of complex [Gd(2)] (ESI-HRMS, negative mode), with characteristic isotopic distribution.

As mentioned above, the complex obtained could not be recrystallized in such a way as to be able to obtain its structure by x-ray. This led us to obtain the ground state geometries by molecular mechanic methods. All the potential starting arrangements of the donor atoms around the Gd (III) metal ion for ligand **2**³⁻, $q = 9$ and a variable number of coordinated water molecules $n\text{H}_2\text{O}$ where n varies from 0 to 3 were considered. Possible donor atoms were defined according to the atomic charges calculated using the NPA scheme [19] and the COSMO model (conductor-like screening solvation model) as implemented in Gaussian09 [28], considering water as a solvent.

The resulting structures were then refined using quantum chemical semiempirical methods, giving rise to a set of low-energy structures.

For molecular mechanics calculations, an extension of the MM+ force field for Gd (III) complexes was used [21].

Semiempirical molecular orbital calculations use the Spar-kle/PM6 method [22], a computational chemistry model faster than *ab initio*/ECP calculations [30], with a comparable accuracy for ligands with directly coordinating nitrogen and/or oxygen atoms [31]. It is noteworthy that regardless of whether the structure of the complex responds to the form [Gd(2)] or [Gd(2)(H₂O)], the ligand has three independent components of chirality, N-C-C-N torsion angle of the chelate ring, the helicity of the side arms. Depending on the sign of the N-C-C-N torsion angle, the conformation of each ethylene group in the macrocyclic ring can be either left-handed, designated as λ (negative N-C-C-N torsion angle), or right-handed, designated as δ (positive N-C-C-N torsion angle), the orientation of the pendant arms can be either clockwise, (positive N-C-C-O torsion angle), or counter-clockwise, Λ (negative N-C-C-O torsion angle). The third independent component of chirality is generated by the orientation of the side arms (SAs) (-CH₂COO-) respect to the surface which contains the Gd nucleus, and whose vertexes were defined by the nuclei **O38-39** and **N2-4**. The description of this property will be represented by the following nomenclature: if two arms joined to two contiguous nuclei of N are on the same side of the surface described, they will be called *syn*(SAsN_n,N_{n+1}), whereas if they are oriented on oppo-site sides, they will be called *anti*(SAsN_n,N_{n+1}). Fig. (6) shows the two minimal energy geometries of complexes [Gd(2)] and [Gd(2)(H₂O)], calculated with PM6/Sparkle and implemented in the program MOPAC2012.

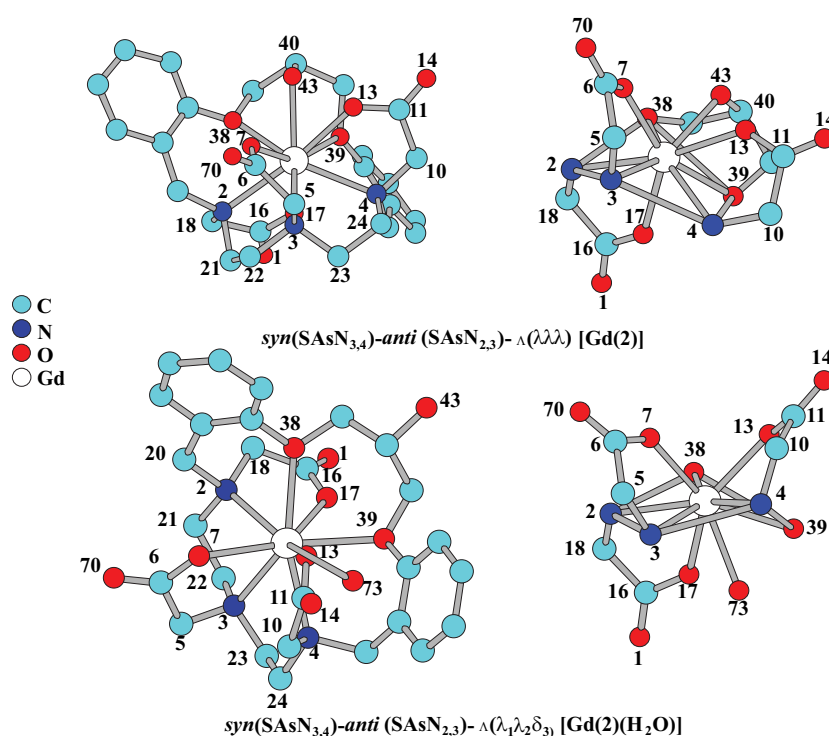


Fig. (6). Minimal energy geometries of complexes [Gd(2)] and [Gd(2)(H₂O)], calculated with PM6/Sparkle.

Also, the fact that the ninth position ($q = 1$) in the latter complex is occupied by the oxygen of a water molecule (**O73**) would make the complex more stable due to a decrease in the effect of electronic repulsion and steric hindrance (which would be comparatively higher in the case of the first complex), wherein the ninth coordinating position ($q=0$) of the Gd (III) is occupied by the oxygen nucleus **O43** corresponding to the hydroxyl group located at **C40**.

“Points on a Sphere” repulsion calculations incisively identify the geometry most favorable polytopal form for an ML9 coordination complex, which will be discussed later [32].

The IR spectrum of each optimized structure was calculated by PM6/Sparkle and AM1/Sparkle models implemented in MOPAC, and Hartree-Fock method. The best results were obtained with the latter method using the with 6-31G basis set and, we applied a quasi-relativistic ECP as described by Dolg *et al.* for the metal atom [30].

The signals on which special attention was given were those that would allow proposing which are the oxygen atoms corresponding to the Ar-O-CH₂ vibrations and $\nu(\text{C-O})$ stretching of the alcohol groups [11, 28, 29, 33]. In this sense, the area of the $\nu(\text{C}=\text{O})$ vibration modes was also analyzed to understand the most probable geometry for the formation of the -COO-Gd bonds (Fig. 7a).

The experimental spectra did not allow verifying the existence or not of the interaction of the tertiary amino groups with Gd, because the area in the spectrum in which the signals corresponding to the stretching vibrations of the bonds C-N (1210-1150 cm⁻¹, N not coordinated) [34] were observed was similar to that in which the signals of the stretches of groups such as Ar-O-C- and -C-OH were observed. In addition, it should not be forgotten that the comparative analysis of the infrared spectra performed was based on the spectrum of the ligand in its salt form Fig. (7b). Considering that the amino groups may be some of those having the greatest interaction with the trifluoroacetate counter ion, precautions should be taken when comparing the observed variations of the functional groups before the formation reaction of the coordination compound, and the spectrum obtained therefrom the latest. However, the analysis of the modes of vibration calculated by computational tools indicates that the tertiary amino groups are coordinating a Gd (III) (Fig. 7b).

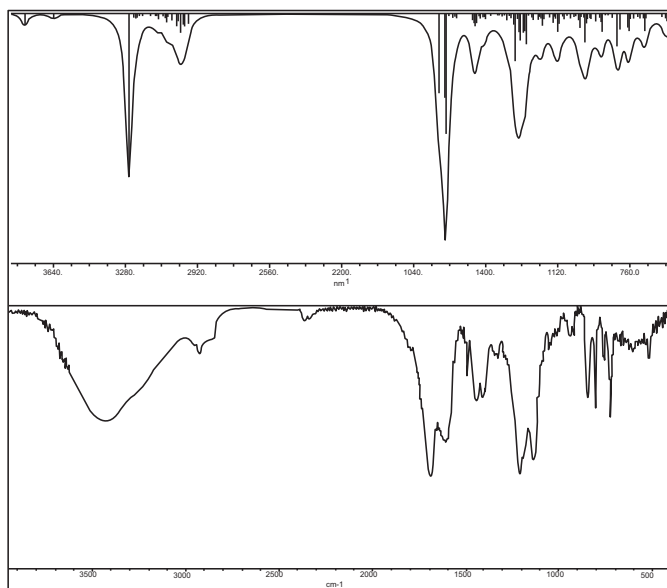


Fig. (7a). Comparison of simulated (upper) versus experimental (bottom) FT-IR for [Gd(2)(H₂O)].

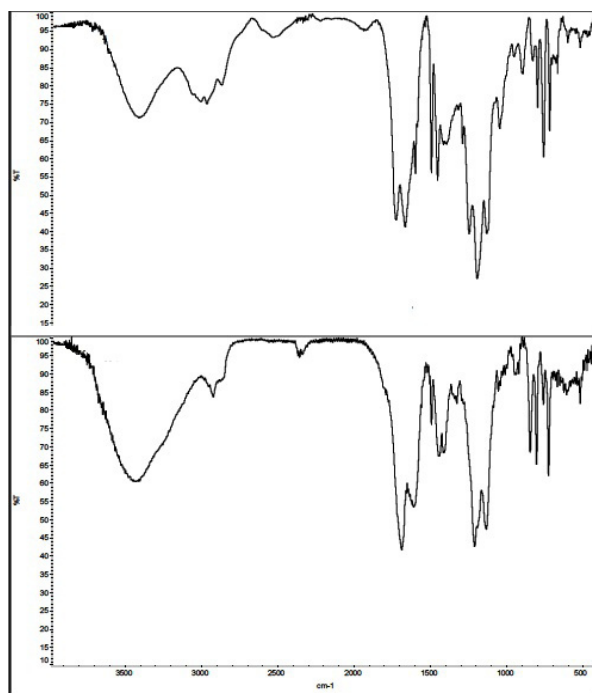


Fig. (7b). FTIR spectra of compound ([2-F₃CCOOH]•H₂O) (upper) and complex and complex [Gd(2)(H₂O)_n] (bottom).

After checking the stoichiometry of complex formed by ligand **2** and Gd (III) by mass spectrometry and being able

to propose the most probable structure from computational calculations and the comparison of the experimental infrared spectra with those obtained for the different geometries calculated from the theoretical tool mentioned above, we decided to perform a comparative analysis of different geometric parameters of the proposed structure with those reported for different complexes of different lanthanides whose CN = 9. The analysis of x-ray data allowed concluding that the observed geometry of many Gd (III) complexes with the CN mentioned above gives rise to a nine coordinated distorted tricapped trigonal prism (D_{h3} geometry) [32]. In the geometry of other complexes, such as Gadobutrol, the coordination polyhedron can be approximated by a distorted monocapped square antiprism (C_{4v}) symmetry [35].

Fig. (7c) shows an enlargement of the regions of the experimental infrared spectra of compound $[2-F_3CCOOH] \cdot H_2O$ and complex $[Gd(2)(H_2O)]$ where the most important differences can be verified and which would allow to make some of the affirmations previously made.

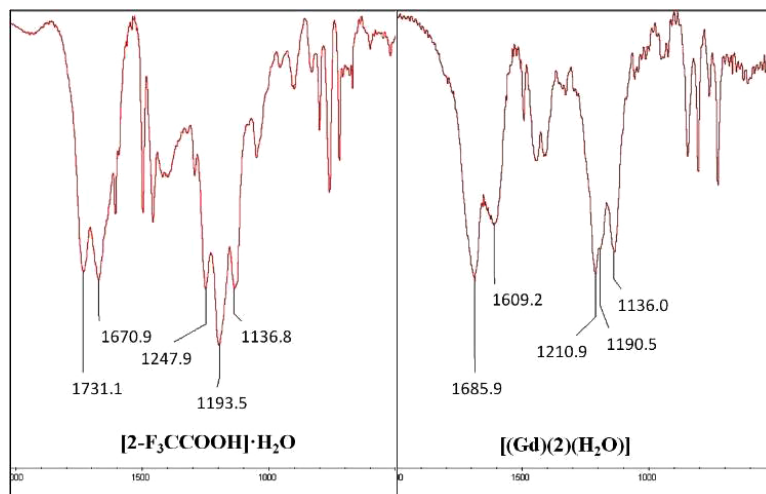


Fig. (7c). Regions FTIR spectra of compound $([2-F_3CCOOH] \cdot H_2O)$ (upper) and complex and complex $[Gd(2)(H_2O)_n]$ (bottom).

As indicated earlier, the theoretical basis to determine the structure of the $[Gd(2)(H_2O)]$ complex was based on “Points on a Sphere” repulsion calculations [32]. The polyhedron corresponding for the most probable structures of the complex obtained is shown in Fig. (8a). Fig. (8b) shows that the capping positions are occupied by the N3 nitrogen atom and the O13 and O17 oxygen atoms of the polyaminopolycarboxylate ligand, while that the vertices of the two triangular faces of the coordination polyhedron are constituted by O73 (Ow), O4, O39 and O38, O7 and N2, respectively. Fig. (8c) intends to show the D_{h3} geometry.

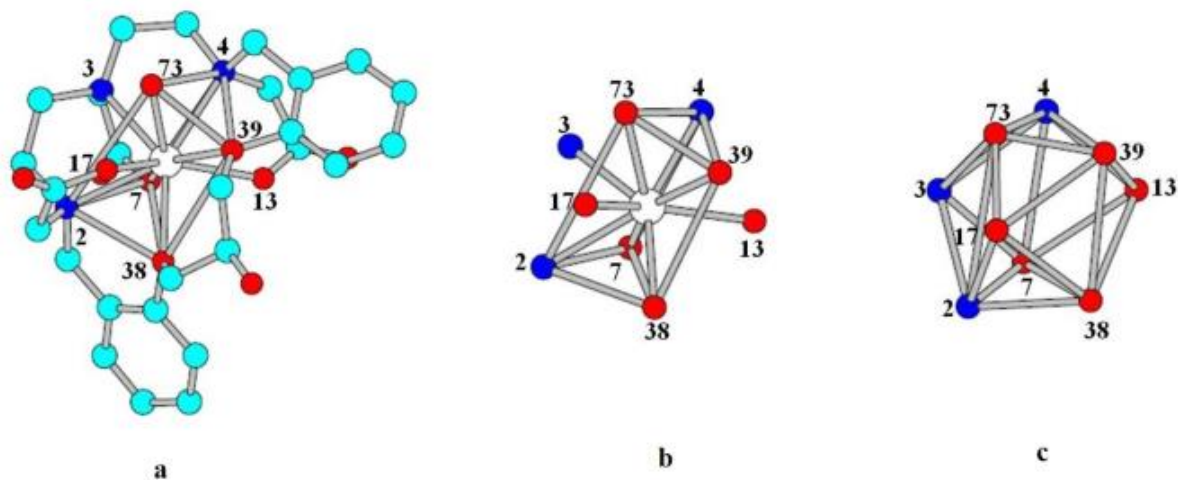


Fig. (8). a) the most probable structures of the complex, b) graphical representation of positions occupied by the heteroatoms of ligand, c) Coordination polyhedron showing D_{h3} geometry.

Table 2 shows selected bond lengths, bond angles and torsion angles for [Gd(2)(H₂O)] complexes, which allowed a comparative analysis with the same parameters reported for other lanthanide complexes with a CN = 9.

The observation of the geometric data of the structure proposed for the [Gd(2)(H₂O)] complex allows stating that Gd (III) is not found in the center of the polyhedron but closer to the faces formed by the atoms **O7-O38-O39-N4** and **N1-N3-O7-O(W)73**, and capped by the atoms **O13**, **O17** and **N3**, respectively.

The average length of Gd-O carboxylate and the bond angles are similar to those previously reported for other Gd (III) complexes [27a, 36] In this same sense, the calculated lengths of the bonds between the cation and the oxygen atoms of the ether bridges were not significantly different from those of other complexes whose ligands are crown ethers. The same parameter for Gd-N bonds was lower than those reported for both complexes whose ligands are cyclic or acyclic [11, 27a]. Regarding the Gd-O water distance, it was practically the same as that found experimentally for different Gd complexes with q = 1 [38].

The torsion angles presented in the table confirm the pro-posed configuration shown in Fig. (8a).

Table 2. Distances and bond/torsion angles, involving the central nine-coordinated Gd (III) atom.

Atoms	Bond Length (Å)	Atoms	Bond Angles (°)	Atoms	Torsion Angles (°)
Gd-O13	2.359	O38-Gd-O39	81.4	N4-C-C-N3	-54.82
Gd-O7	2.373	N2-Gd-N3	71.55	N3C-C-N2	55.12
Gd-O17	2.393	N2-Gd-N4	141.66	N3-C-C-O13	27.14
Gd-O38	2.472	N3-Gd-N4	70.32	N2-C-C-O17	-23.59
Gd-O39	2.513	O7-Gd-O13	84.04	N1-C-C-O3	-33.83
Gd-O(W)73	2.451	O13-Gd-O17	136.22		
Gd-N1	2.550	O17-Gd-O7	133.33		
Gd-N2	2.512	N2-Gd-O7	70.34		
Gd-N3	2.532	N2-Gd-O13	139.92		
C-O13	1.297	N2-Gd-O17	63.27		
C-O7	1.287	N3-Gd-O7	64.38		
C-O17	1.316	N3-Gd-O13	124.48		
Ph-O38	1.429	N3-Gd-O17	96.96		
C-O38	1.478	N4-Gd-O7	89.62		
Ph-O39	1.432	N4-Gd-O13	64.78		
C-O39	1.476	N4-Gd-O17	124.76		
		C-C-O7	111.24		
		C-C-O13	110.49		
		C-C-O17	109.78		

When evaluating the information obtained from computational calculations, it must be taken into account that the structure obtained and proposed as the most probable was estimated in gaseous state. This is important to consider since there is experimental evidence that, in solution, the Gd (III) complexes derived from cyclic ligands suffer from structural changes due to the inversion of the ring and rotation of the arms [27a, 38].

CONCLUSIONS

Our first objective was to optimize the synthesis of intermediates **3** and **4** using microwave irradiation. In the case of compound **3**, the reaction medium was an excess of salicylaldehyde as a solvent. The work up was simpler and more environmentally friendly, since the excess aldehyde was recovered by distillation under reduced pressure. Regarding the alkylation stage of the amino groups, the most notable improvement was the reduction of the reaction time.

Subsequently, we analyzed the effects of different experimental parameters on r_1 . The most important effect was generated by the variation of the pH (an inflection point was observed approximately at 6.5). To verify that the variation of r_1 was not the product of the decomposition of the complex, the solutions containing the Gd (III) complex in different concentrations were subjected to incubency by using a methodology already reported [16]. The results obtained allowed us to conclude that the change in r_1 was reversible.

Next, we attempted to establish whether the hydroxyl group was involved in the coordination sphere of the lanthanide, for which we proposed using computational calculations and comparing which of the geometries obtained corresponded to the coordination compound under study. To obtain results consistent with the real structure of the complex, the theoretical and experimental IR spectra calculated for each of the generated geometries were compared. Based on this information and mass spectrometry data, the most probable structure is isomer SA[Gd(2)(H₂O)], in which Gd (III) has CN = 9, where the ninth position is occupied by a water molecule ($q = 1$).

Another relevant finding was the variation of r_1 as a function of temperature. As we cannot accurately control the aforementioned parameter, we do not report in detail the results observed.

On the other hand, the longitudinal proton relaxivities, measured at 37°C and pH close to the neutrality of **Gd-2**, Gd-DTPA (see Fig. 3) falls in the range of values typical of $q < 1$ and $q = 1$, respectively [27]. This would indicate that the complex has a 9-coordinate ground state with one inner sphere water molecule, at pH 6.5. The occurrence of $q = 1$ excludes the possible involvement of the OH groups of the ligand in the coordination of the metal ion.

Based on all the above, we will continue working with the same ligand, but using the Eu (III) and Tb (III) lanthanides so as to obtain additional information that allows us to understand the form of action of the mentioned complex.

CONSENT FOR PUBLICATION

Not applicable.

CONFLICT OF INTEREST

The authors declare no conflict of interest, financial or otherwise.

ACKNOWLEDGEMENTS

The corresponding author would like to thank Dr. J.P. Stewart for the free use of the MOPAC2012 computer package.

REFERENCES

- [1] (a) Kanal, E. Gadolinium-based magnetic resonance contrast agents for neuroradiology: An overview. *Magn. Reson. Imaging Clin. N. Am.*, **2012**, *20*, 625-631. (b) Schuster, A.; Morton, G.; Chiribiri, A.; Perera, D.; Vanoverschelde, J.L.; Nagel, E. Imaging in the management of ischemic cardiomyopathy: Special focus on magnetic resonance. *J. Am. Coll. Cardiol.*, **2012**, *59*(4), 359-370.

- [2] Arnaud, F.-X.; Hissene, A.; Métivier, D.; Dutasta, F.; Berets, O.; N'Guema, B.; A'Teritiéhou, C.; Baccialone, J.; Potet, J. Gadolinium enhancement in brain magnetic resonance imaging in progressive multifocal leukoencephalopathy after natalizumab monotherapy: Is it really atypical? *J. Neuroradiol.*, **2012**, 39(4), 267-270.
- [3] Troum, O.M.; Pimienta, O.; Olech, E. Magnetic resonance maging applications in early rheumatoid arthritis diagnosis and management. *Rheum. Dis. Clin. North Am.*, **2012**, 38(2), 277-297.
- [4] Banci, L.; Bertini, I.; Luchinat, C. *The magnetic nucleus-unpaired electron coupling in solution*; Wiley-VCH Verlag GmbH: New York, **1991**.
- [5] Kowalewski, J.; Nordenskiöld, L.; Benetis, N.; Westlund, P.O. Theory of nuclear spin relaxation in paramagnetic systems in solution. *Prog. Nucl. Magn. Reson. Spectrosc.*, **1985**, 17, 141-185.
- [6] Grover, V.P.; Tognarelli, J.M.; Crossey, M.M.; Cox, I.J.; Taylor-Robinson, S.D.; McPhail, M.J. Magnetic resonance imaging: Principles and techniques: Lessons for clinicians. *J. Clin. Exp. Hepatol.*, **2015**, 5(3), 246-255.
- [7] (a) Gries, H.; Rosemberg, D.; Weinmann, H.-J.; Speck, U.; Mützel, W.; Hoyer, G.-A.; Pfeiffer, H.; Renneke, F.-J. Gadolinium chelates for magnetic resonance imaging. U.S. Patent 5,362,475, August 08, 1994.(b) Gries, H.; Rosemberg, D.; Weinmann, H.-J.; Speck, U.; Mützel, W.; Hoyer, G.A.; Pfeiffer, H.; Renneke, F.-J. Method of enhancing paramagnetism in chelates for MRI. U.S. Patent 5,560,903, January 10, 1996.(c) Gries, H.; Speck, U.; Weinmann, H.-J.; Nien-dorf, H.P.; Seifert, W. Metal complex- containing pharmaceutical agents. U.S. Patent 5,876,695, February 02, 1999.
- [8] http://www3.gehealthcare.com/en/products/categories/contrast_media/omniscan (Accessed January 30, 2018).
- [9] https://www.accessdata.fda.gov/drugsatfda_docs/label/2006/020937,020975,020976s009lbl.pdf (Accessed January 30, 2018).
- [10] Uggeri, F.; Aime, S.; Anelli, P.L.; Botta, M.; Brocchetta, M.; De Haën, C.; Ermondi, G.; Grandi, M.; Paoli, P. Novel contrast agents for magnetic resonance imaging. Synthesis and characterization of the ligand BOPTA and its Ln(III) complexes (Ln = Gd, La, Lu). X-ray structure of disodium (TPS-9-145337286-C-S)-[4-carboxy-5,8,11-tris(carboxymethyl)-1-phenyl-2-oxa-5,8, 11-triazatridecan-13-oato(5-)]gadolate(2-) in a mixture with its enantiomer. *Inorg. Chem.*, **1995**, 34(3), 633-642.
- [11] Berg, T.; Simeonov, A.; Janda, K.D. A combined parallel synthesis and screening of macrocyclic lanthanide complexes for the cleavage of phospho di- and triesters and double-stranded DNA. *Comb. Chem.*, **1999**, 1(1), 96-100.
- [12] (a) Wike-Hooley, J.L.; Haveman, J.; Reinhold, J.S. The relevance of tumour pH to the treatment of malignant disease. *Radiother. Oncol.*, **1984**, 2(4), 343-366.(b) Vaupel, P.; Kallinowski, F.; Oku-nieff, P. Blood Flow, oxygen and nutrient supply, and metabolic microenvironment of human tumors: A review. *Cancer Res.*, **1989**, 49(23), 6449-6465.(c) Gerweck, L.E.; Sheetharaman, K. Cellular pH gradient in tumor versus normal tissue: Potential exploitation for the treatment of cancer. *Cancer Res.*, **1996**, 56(6), 1194-1198.(d) Ballesterosa, P.; Pérez-Mayoral, E.; Benitoc, M.; Cerdánc, S. Magnetic resonance imaging and magnetic resonance spectroscopy methods for measuring intra and extra-cellular pH: clinical implications. *Radiología*, **2008**, 50(6), 463-470; <http://www.elsevier.es/es-revista-radiologia-119-linkresolver-spec-troscopia-e-imagen-del-ph-131-29445>;(e) Sennoune, S.R.; Luo, D.; Martinez-Zaguilan, R. Plasmalemmal vacuolar-type H⁺-ATPase in cancer biology. *Cell Biochem. Biophys.*, **2004**, 40(2), 185-206.(f) Tannock, I.F.; Rotin, D. Acid pH in tumors and its potential for therapeutic exploitation. *Cancer Res.*, **1989**, 49(16), 4373-4384. [Rustoy and Raggio].
- [13] (a) Pfeuffer, J.; Mishra, A.; Logothetis, N.K. Design, synthesis and characterization of new smart MR contrast agents sensitive to pH. *Proc. Intl. Soc. Magn. Reson. Med.*, **2005**, 13, 2582.(b) Zhang, S.; Wu, K.; Sherry, A.D. A novel pH-responsive MRI contrast agent. *Angew. Chem., Int. Ed.*, **1999**, 38(21), 3192-3194.(c) Kálmán, F.; Woods, M.; Caravan, P.; Jurek, P.; Spiller, M. Potentiometric and relaxometric properties of a gadolinium-based MRI contrast agent for sensing tissue pH. *Inorg. Chem.*, **2007**, 46(13), 5260-5270.(d) Aime, S.; Barge, A.; Castelli, D.D.; Fedeli, F.; Mortillaro, A.; Nielsen, F.U. Paramagnetic lanthanide(III) complexes as pH-sensitive Chemical Exchange Saturation Transfer (CEST) contrast agents for MRI applications. *Magn. Reson. Med.*, **2002**, 47(4), 639-648.(e) Lokling, K.E.; Skurtveit, R.; Bjornerud, A.; Fossheim, S.L. Novel pH-sensitive paramagnetic liposomes with improved MR properties. *Magn. Reson. Med.*, **2004**, 51(4), 688-696.(f) Xu, Q.; Liu, L.; Zhu, L.; Yu, M.; Yang, Q.; Wang, S. A conjugated polymer - Gd (III) complex as pH sensitive contrast agent in magnetic resonance imaging. *Front. Chem. China.*, **2010**, 5(2), 166-170.(g) Kim, K.S.; Park, W.; Hu, J.; Bae, Y.H.; Na, K. A cancer-recognizable MRI contrast agents using pH-responsive polymeric micelle. *Biomaterials*, **2014**, 35(1), 337-343.(h) Iwaki, S.; Hanaoka, K.; Piao, W.; Komatsu, T.; Ueno, T.; Terai, T.; Nagano, T. Development of hy-poxia-sensitive Gd³⁺-based MRI contrast agents. *Bioorg. Med. Chem. Lett.*, **2012**, 22(8), 2798-2802.
- [14] Louie, A. MRI biosensors: A short primer. *J. Magn. Reson. Imag-ing*, **2013**, 38(3), 530-539; (b) Sherry, A.D.; Woods, M. Chemical exchange saturation transfer contrast agents for magnetic resonance imaging. *Annu. Rev. Biomed. Eng.*, **2008**, 10, 391-411. [and refer-ences therein.].
- [15] Martínez, M.D.; Rustoy, E.M.; Raggio, N.; Burton, G. Synthesis and characterization of a new polyaminocarboxylic macrocyclic ligand and its nonion gadolinium complex. *in vitro* relaxivity stud-ies at 0.2 T. *Inorg. Chem. Commun.*, **2015**, 51, 110-113.
- [16] Woods, M.; Kiefer, G.E.; Bott, S.; Castillo-Muzquiz, A.; Eshelbrenner, C.; Michaudet, L.; McMillan, K.; Mudigunda, S.D.K.; Ogrin, D.; Tircsó, G.; Zhang, S.; Zhao, P.; Sherry, A.D. Synthe-sis, relaxometric and photophysical properties of a new pH-responsive MRI contrast agent: The effect of other ligating groups on dissociation of a p-nitrophenolic pendant arm. *J. Am. Chem. Soc.*, **2004**, 126(30), 9248-9256.
- [17] Wong, K.; Ananta, J.S.; Patz, S.; Muradyan, I.; Wilson, L.J. *In vitro* relaxivities studies of gadolinium carbon nanotubes at 0.2 T. *Proc. Int. Soc. Magn. Reson. Med.*, **2008**, 16, 1664.
- [18] Becke, A.D. Density functional thermochemistry. III. The role of the exact exchange. *J. Chem. Phys.*, **1993**, 98(7), 5648-5652.
- [19] Kostova, I.; Trendafilova, N.; Momekocv, G. Theoretical, spectral characterization and antineoplastic activity of new lanthanide complexes. *J. Trace Elem. Med. Biol.*, **2008**, 22, 100-111. [and refer-ences therein.].

- [20] Frisch, M.J.; Trucks, G.W.; Schlegel, H.B.; Scuseria, G.E.; Robb, M.A.; Cheeseman, J.R.; Scalmani, G.; Barone, V.; Mennucci, B.; Petersson, G.A.; Nakatsuji, H.; Caricato, M.; Li, X.; Hratchian, H.P.; Izmaylov, A.F.; Bloino, J.; Zheng, G.; Sonnenberg, J.L.; Hada, M.; Ehara, M.; Toyota, K.; Fukuda, R.; Hasegawa, J.; Ishida, M.; Nakajima, T.; Honda, Y.; Kitao, O.; Nakai, H.; Vreven, T.; Montgomery, J.A.; Peralta, J.E.; Ogliaro, F.; Bearpark, M.; Heyd, J.J.; Brothers, E.; Kudin, K.N.; Staroverov, V.N.; Kobayashi, R.; Normand, J.; Raghavachari, K.; Rendell, A.; Burant, J.C.; Iyengar, S.S.; Tomasi, J.; Cossi, M.; Rega, N.; Millam, J.M.; Klene, M.; Knox, J.E.; Cross, J.B.; Bakken, V.; Adamo, C.; Jaramillo, J.; Gomperts, R.; Stratmann, R.E.; Yazyev, O.; Austin, A.J.; Cammi, R.; Pomelli, C.; Ochterski, J.W.; Martin, K.; Morokuma, V.G.; Zakrzewski, G.A.; Voth, S.P.; Dannenberg, J.J.; Dapprich, S.; Daniels, A.D.; Farkas, O.; Foresman, J.B.; Ortiz, J.V.; Cioslowski, J.; Fox, D.J. Gaussian09. Wallingford, CT: Gaussian Inc., 2009. p. A.2; Gaussian 09, Revision A.02.
- [21] <http://www.sparkle.pro.br/tutorial/drawing-complexes> (Accessed February 02, 2018).
- [22] (a) Stewart, J.P. **2018**. MOPAC2012, Stewart Computational Chemistry, Version 15.301W web: [HTTP://OpenMOPAC.net](http://OpenMOPAC.net) (Accessed February 02, 2018)(b) Maia, J.D.C.; Carvalho, G.A.U.; Mangueira, C.P., Jr; Santana, S.R.; Cabral, L.A.F.; Rocha, G.B. GPU linear algebra libraries and GPGPU programming for accelerating MOPAC semiempirical quantum chemistry calculations. *J. Chem. Theory Comput.*, **2012**, 8(9), 3072-3081.
- [23] Allouche, A.R. Computational Chemistry Softwares. *J. Comput. Chem.*, **2011**, 32, 174-182.
- [24] (a) Zhao, B.; Wu, Y.J. Tao, on the syntheses of hydroxy - bearing benzo - azacrown ethers and their complexing behaviour. *Polyhedron*, **1996**, 15(7), 1197-1202.(b) Abbas, A.A. cles containing two Triazole rings and bis crown macrocycles containing four triazole rings. *Tetrahedron*, **2004**, 60(7), 1541-1548.(c) Khalil, N.S. acyclic and 21-28 membered macrocyclic and/or lariat macrocyclic oxazathia crown compounds with potential antimicrobial activity. *Eur. J. Med. Chem.*, **2010**, 45(11), 5265-5277.
- [25] Gabriel, C.; Gabriel, S.; Grant, E.H.; Halstead, B.S.J.; Mingos, D.M.P. Dielectric parameters relevant to microwave dielectric heating. *Chem. Soc. Rev.*, **1998**, 27(3), 213-224.
- [26] Larhed, M.; Moberg, C.; Hallberg, A. *Acc. Chem. Res.*, **2002**, 35(9), 717-727.
- [27] (a) Caravan, P.; Ellison, J.J. McMurry, linium (III) chelates as MRI contrast agents: structure, dynamics, and applications. *Chem. Rev.*, **1999**, 99, 2293.(b) Aime, S.; Botta, M.; Terreno, E. Gd (III)-based contrast agents for MRI in advances in inorganic chemistry; R. van Eldik and I. Bertini, Eds.; Elsevier: San Diego, 2005; Vol. 57, pp. 173-237.
- [28] Berg, T.; Vandersteen, A. M.; Janda, K.D. High-throughput synthesis and direct screening for the discovery of novel hydrolytic metal , **1998**, 8(10), 1221-1224.
- [29] Liu, J-L.; Yan, B. Lanthanide-centered organicinorganic hybrids through a functionalized. Aza-Crown Ether Bridge: Coordination bonding Assembly, microstructure and multicolor luminescence. *Dalton Trans.*, **2011**, 40(9), 1961-1968.
- [30] Dolg, M.; Stoll, H.; Savin, A.; Preuss, H. Energy-adjusted pseudo- potentials for the rare-earth elements. *Theor. Chim. Acta*, **1989**, 75(3), 173-194.
- [31] Daniel, C.R.A.; Rodrigues, N.M.; da Costa, N.B. Are quantum chemistry semiempirical methods effective to predict solid state structure and adsorption in metal organic frameworks? *J. Phys. Chem. C*, **2015**, 19(41), 23398-23406.
- [32] Guggenberger, L.J.; Muetterties, E.L. Reaction path Analysis. 2. The nine-atom family. *J. Am. Chem. Soc.*, **1976**, 98(3), 7221-7225.
- [33] (a) Eisenstein, O.; Maron, L.J. DFT Studies of some structures and reactions of lanthanides complexes. *Organomet. Chem.*, **2002**, 647(1-2), 190-197.(b) Cao, X.; Dolg, M. Density functional studies on lanthanide (III) texaphyrins (Ln- Tex^{2+}), Ln = La, Gd, Lu): Structure, stability and electronic excitation spectrum. *Mol. Phys.*, **2009**, 101(15), 2427-2435.(c) Cosentino, U.; Villa, A.; Pitea, D.; Moro, G.; Barone, V.; Maiocchi, V. Conformational characterization of lanthanide(III)-DOTA complexes by ab Initio investigation in vacuo and in aqueous solution. *J. Am. Chem. Soc.*, **2002**, 124(17), 4901-4909.(d) Perrin, L.; Maron, L.; Eisenstein, O. Modelling Me5C5 for reactivity studies in (Eta(5)-C5Me5)(2)Ln-R: full DFT and QM/MM approaches. *New J. Chem.*, **2004**, 28(10), 1255-1259.(e) Pérez-Mayoral, E.; Soriano, E.; Cerdán, S.; Ballesteros, P. Experimental and theoretical study of lanthanide complexes based on linear and macrocyclic polyaminopolycarboxylic acids containing pyrazolyethyl arms. *Molecules*, **2006**, 11(5), 345-356.
- [34] Coates, J. Interpretation of infrared spectra, A practical approach. Encyclopedia of Analytical Chemistry, 2006, 1.
- [35] Platzek, J.; Blaszkiewicz, P.; Gries, H.; Luger, P.; Michl, G. Muller-Fahrnow, A.; Radulchel, B.; Sulzle, D. Synthesis and structure of a new macrocyclic polyhydroxylated gadolinium chelate used as a contrast agent for magnetic resonance imaging. *Inorg. Chem.*, **1997**, 36(26), 6086-6093.
- [36] Grenthe, J. Structural studies on the rare Earth carboxylates. 14. A structural study of the orthorhombic trishydroxyacetates of Lanthanum(III) and Gadolinium(III). *Acta Chem. Scand.*, **1972**, 26, 1479-1489.
- [37] Willey, G.R.; Woodman, T.J.; Drew, M.G.B. Lanthanide(III) chloride-tetrahydrofuran solvates: Structural patterns within the series $\text{LnCl}_3(\text{THF})_n$, where $n = 2, 3, 3.5$ and 4: Crystal and molecular structures of $[\text{PrCl}(\text{THF})_2]_n$, $[\text{Nd}(\text{H}_2\text{O})(\text{THF})]_n$ and $\text{GdCl}_3(\text{THF})_4$. *Polyhedron*, **1997**, 16(19), 3385-3393.

- [38] (a) Parker, D.; Dickins, R.S.; Puschmann, H.; Crossland, C.; Howard, J.A.K. Being excited by lanthanide coordination complexes: aqua species, chirality, excited-state chemistry, and exchange dynamics. *Chem. Rev.*, **2002**, *102*(6), 1977-2010.

© 2018 Rustoy and Raggio.

This is an open access article distributed under the terms of the Creative Commons Attribution 4.0 International Public License (CC-BY 4.0), a copy of which is available at: <https://creativecommons.org/licenses/by/4.0/legalcode>. This license permits unrestricted use, distribution, and reproduction in any medium, provided the original author and source are credited.